RoboTwin

A Platform to Study Hydrodynamic Interactions in Schooling Fish

By Liang Li ⓘ, Li-Ming Chao ⓘ, Siyuan Wang ⓘ, Oliver Deussen ⓘ, and Iain D. Couzin ⓘ

By living and moving in groups, fish can gain many benefits, such as heightened predator detection, greater hunting efficiency, more accurate environmental sensing, and energy saving. Although the benefits of hydrodynamic interactions in schooling fish have drawn growing interest in fields such as biology, physics, and engineering, and multiple hypotheses for how such benefits may arise have been proposed, it is still largely unknown which mechanisms fish employ to obtain hydrodynamic benefits, such as increased thrust or improved movement efficiency. One main bottleneck has been the difficulty in collecting detailed sensory information, corresponding locomotory responses, and hydrodynamic information from real schooling fish.

In this article, we present the RoboTwin platform designed to aid in such data collection; it allows us to replay the dynamic movements and body posture kinematics of real fish in fishlike robots, allowing us to measure the power cost, thrust, and detailed flow fields, all of which are extremely challenging to collect from real animals. To mutually verify the capabilities of our platform and our previously proposed mechanism of energy saving ("vortex phase matching"), we reanalyzed two goldfish (*Carassius auratus*) swimming in a flow tank, from which dynamic positions and corresponding body kinematics are quantified. By employing the RoboTwin system, we find that there exist notable benefits to swimming together (for the kinematic patterns exhibited by real fish pairs), both in energy saving (approximately 8%) and in thrust enhancement (around 35%), compared to when swimming alone. Flow visualization through particle image velocimetry (PIV) shows that energy savings arise due to vortex phase matching. Our results demonstrate the effectiveness of our design and highlight the potential of RoboTwin for future applications in exploring further hydrodynamic interactions among schooling fish.

INTRODUCTION

Collective animal behavior is a complex and intriguing phenomenon observed in various species on our planet [1], [2]. By moving collectively, individuals can benefit in many ways, including improved predator avoidance, increased foraging efficiency, accurate environmental sensing, and energy saving [1], [3]. Uncovering what kinds of benefits fish gain when they swim in groups has drawn great attention from many disciplines, including biology, physics, mathematics, and engineering.

The possibility of saving energy by swimming together has been of particular interest in collective fish behavior [4]. Although it is thought that fish may be able to extract energy from vortices shed by neighbors, with support coming from theoretical modeling [4], simulations [5], [6], and physical models [7] as well as experiments on real fish [8], it is still largely unknown when and how fish save energy given their dynamic kinematics and spatiotemporal movements. Since fish will not always be expected to coordinate movement in such a way as to save energy (e.g., they may also do so to enhance thrust, depending on time-varying behavioral and ecological contexts), we first need an easy and robust way to explore when and how they create—and respond to—socially generated hydrodynamic features. To do so, we need to establish how they adjust their body kinematics and spatiotemporal relationships in schools to extract energy from nearby

> **IT IS STILL LARGELY UNKNOWN WHEN AND HOW FISH SAVE ENERGY GIVEN THEIR DYNAMIC KINEMATICS AND SPATIOTEMPORAL MOVEMENTS.**

vortices. A deep understanding of the behavioral triggers of efficient swimming behavior and sensory-motor control mechanisms of schooling fish might also inspire the design and control of effective underwater robots [9].

One main bottleneck for such understanding has been the difficulty of collecting detailed sensory information and socially generated flow properties from real fish. For example, the direct and indirect estimation of energy cost of a living organism is typically affected by an individual's cognitive responses, such as experiencing greater stress, and thus higher metabolic expenditure, when isolated from others, independent of hydrodynamic interactions [10]. Energy savings are expected to be greater for larger sized schooling fish (their Reynolds number is higher), and especially for fish over long distances. Unfortunately, obtaining detailed sensing and hydrodynamic information using computational fluid dynamics is extremely challenging and computationally expensive in 3D at such high Reynolds numbers [11]. Experimental physical models, such as filaments [7], [12] and rigid foils [13], have been proposed to estimate hydrodynamic interactions in fish schools.

However, such studies ignore the morphology of the fish body despite the fact that it likely plays an important role in the hydrodynamic interactions; furthermore, the precise control of tail movements is sophisticated. Existing robotic fish models [8], [14] are limited to testing hypotheses using
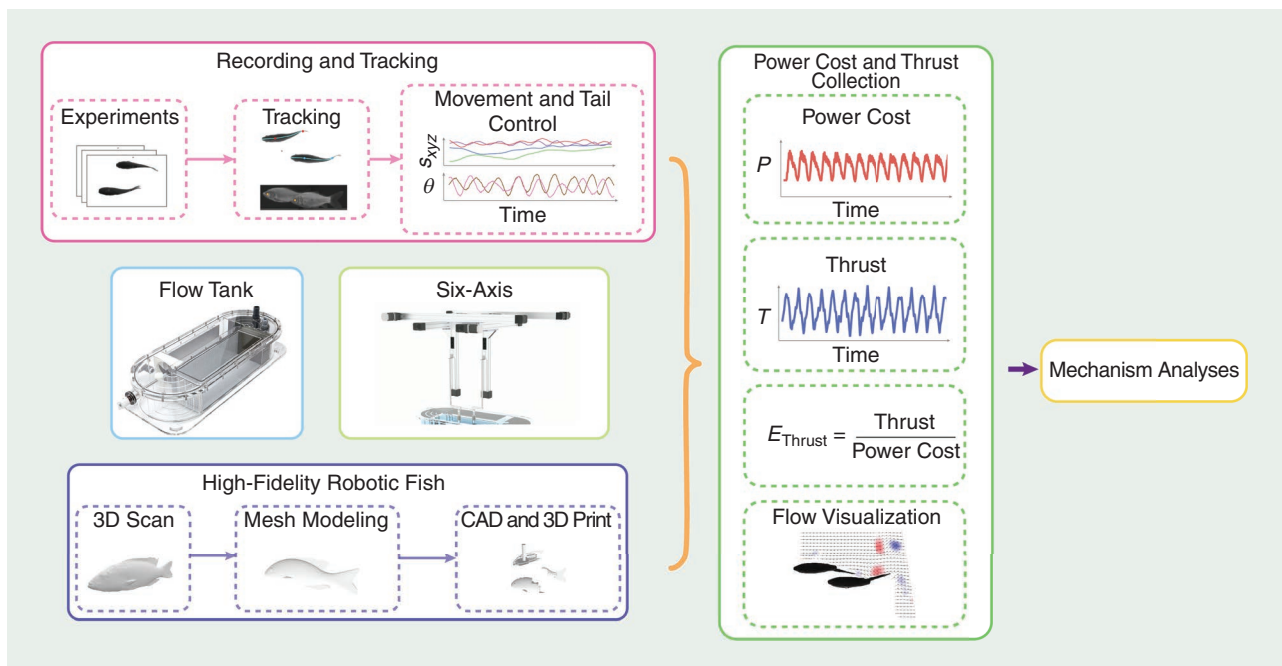

FIGURE 1. A schematic overview of our experiments and design of the RoboTwin platform. It includes a flow tank platform, a recording and tracking system, high-fidelity robotic fish models, a six-axis motion platform, and a power cost and thrust measuring system. All of these ensure that our robotic twins can replay the schooling behavior of real fish, including morphology, movements, and kinematics. Power costs, thrust, thrust efficiency, and flow visualization of the hydrodynamic interaction are collected for further behavioral analysis.

idealized kinematics under simplified spatiotemporal formations, such as those with fixed spatial formations and phase differences. In contrast, real fish dynamically alter their body kinematics and spatiotemporal formations. Overall, most existing studies tend to oversimplify the situation as they employ only very limited real fish data for morphology, movements, and tail undulations.

In this article, we present a RoboTwin platform to study hydrodynamic interactions in fish schools. Contrary to our previous models [8], [14], which could gather only the average power costs and thrusts of robots over fixed spatiotemporal formations, the robotic twins of schooling fish enable us to replicate the morphology, dynamic spatiotemporal movements, and instantaneous body kinematics displayed by real fish. To do so, our platform includes a flow tank system, a recording and tracking system, high-fidelity robotic fish models, a six-axis position control system for multiple individuals, and a power and thrust measurement system (see Figure 1). The flow tank allows real fish to swim in a relatively stable formation for long periods of time. The recording and tracking system collects videos of the fish, from which we extract detailed positional and kinematic information in 3D. These data can then be utilized to recreate the motion and postural changes of the robotic twins. To capture the main features of their morphology, we created high-fidelity robotic fish models based on 3D scans of the species under study, thus allowing realistic flow fields to be generated around the robotic fish. The six-axis system is designed to allow the robotic fish to move in 3D. The power and thrust measurement system is designed to collect detailed quantification of the power costs and forces experienced by each of two robotic fish twins swimming in the flow tank. We further present experiments with two goldfish (*Carassius auratus*) to demonstrate how we quantify the movements and kinematics of real fish and then implement these same spatiotemporal properties in our robotic twins to evaluate detailed power costs and thrust properties, which are very difficult to obtain from living animals.

DESIGN OF THE PLATFORM

The main design objective of this platform is to provide us with an easy-to-use and powerful physical model of real fish to collect detailed hydrodynamic information, allowing the investigation of how fish sense and obtain energetic benefits when schooling. Figure 1 illustrates the main modules of the platform. To create robotic fish with appropriate morphology, we 3D-scan the fish bodies (goldfish, *Carassius auratus*) used in the experiments. To obtain the detailed movements and kinematics for driving the robots to move and exhibit tailbeat dynamics similar to real fish, we first ran experiments with real animals within a flow tank, tracking their positions and estimating their time-varying postures by

> **"TO CAPTURE THE MAIN FEATURES OF THEIR MORPHOLOGY, WE CREATED HIGH-FIDELITY ROBOTIC FISH MODELS BASED ON 3D SCANS OF THE SPECIES UNDER STUDY."**

employing deep learning [15]. In this way, we obtained the data needed to control the robotic twins. Replaying the biological kinematics in our robots swimming in a group and alone allowed us to extract power costs and thrusts, and subsequently, to estimate the benefit of swimming in groups for each robotic twin.

FLOW TANK

We performed experiments in a flow tank (Loligo system, Tjele, Denmark) at the Max Planck Institute of Animal Behavior in Konstanz, Germany. The effective test area of the flow tank is 0.25 m wide, 0.875 m long, and 0.25 m deep. The speed of the laminar flow is controlled by a three-phase motor, with rotation speed controlled by a voltage signal. Before experiments, we first calibrated the flow speed with a vane wheel flow probe (Höntzsch, Germany).

THE RECORDING AND TRACKING SYSTEM

A mirror was positioned below the tank at an angle of 45° with respect to the horizontal plane to allow the camera to record the bottom view. Bottom-view and lateral-view cameras (BASLER acA2000-165umNIR, Germany) were used to film fish movements at 100 frames/s. The resolution was set to 2,048×1,058. Videos were recorded using a custom commercial setup (Loopbio, Austria). The tracking was conducted from the bottom and side views based on deep learning algorithms [15], [16]. DeepLabCut [16] was first used to detect each fish's nose and left eye from the bottom-view and side-view videos, respectively. Utilizing the detected nose positions, we applied a Kalman filter and a simple greedy algorithm to track each fish. Based on the tracked positions, we cropped each fish and conducted posture tracking with the software DeepPoseKit [15]. Figure 2 presents a snapshot of the experimental design, detailing extracted spatiotemporal information in schooling fish. This includes tail tip movements L_t, the phase ϕ of the tail tip movements, the phase difference Φ between the two fish, the left–right distance G, and the front–back distance D. Our tracking system captures detailed 3D movement and reconstructs the mesh of the fish body over time [17]. However, given that fish exhibit the strongest hydrodynamic interactions during 2D swimming, this study concentrates mainly on interactions along the x- and y-axes, excluding data from the z-axis.

ROBOTIC FISH

Our robotic fish models were designed according to the morphology of the real fish. We first scanned real fish to obtain the 3D fish body as a point cloud map. Reverse modeling of the mesh from the cloud map was utilized for our mechanical design using SolidWorks. Subsequently, the fish body was 3D-printed using an Ultimaker S3 printer with

polylactic acid material, while the soft tail was printed using TPU 95 A (thermoplastic polyurethane). Limited by the size of the real fish, we included a single joint in this robot design. However, multiple-jointed fish models will be evaluated in our future studies. The oscillation of this joint is controlled by a waterproof servomotor (Hitec HS-5086WP) driven by a central pattern generator (CPG) control [18]. Using the CPG, we can precisely control the robots' tailbeats synchronously with their 3D position by inputting kinematics extracted from the real fish system.

SIX-AXIS MOTION PLATFORM

Due to the limitations of motors and materials of the robotic fish body, it is still not possible to utilize free-swimming robots to replay the movements and body kinematics of real fish. To closely replicate the characteristics of real fish, we developed a six-axis platform to maneuver two robotic fish within the flow tank along the *x*-, *y*-, and *z*-axes. Each of these axes independently controls the respective *x*-, *y*-, or *z*-movement for each robot (see supplementary video for details). The *x*-, *y*-, and *z*-axis controls are mediated by three step motors. The motors are controlled by Arduinos (Mega 2560), which receive the positional information obtained by the experiments with the real fish from a server PC and control all step motors synchronously. The location of the robot in space is updated every 100 ms based on the tracked fish positions. Overall, the robotic fish are able to move similarly to how the real fish did in the flow tank in 3D (except for the orientation control, assuming that rheo-

> **THE MAIN DESIGN OBJECTIVE OF THIS PLATFORM IS TO PROVIDE US WITH AN EASY-TO-USE AND POWERFUL PHYSICAL MODEL OF REAL FISH TO COLLECT DETAILED HYDRODYNAMIC INFORMATION.**

taxis behavior in laminar flow maintains a fixed orientation against the flow). To avoid collisions, we have a brake safety system that stops the system when the two robots get too close.

POWER COST AND THRUST MEASURING SYSTEM

Following our previous studies [8], [14], we estimate the power cost by measuring the current (NI 9227, National Instruments) while the robot is powered by a constant voltage power supply. We set the data acquisition rate as 5.000 samples per second to reduce the effect of noise. To estimate the power cost due to hydrodynamics and to exclude mechanical energy conversion loss as well as thermal energy conversion loss, we first measure the power cost of the robot swimming in the air P_{air}, and subtract this from the power cost under the water P_{water}, to get the power cost due to the hydrodynamics P_{hydro},

$$P_{hydro} = P_{water} - P_{air}. \qquad (1)$$

To measure the thrust, we installed a load cell (HBM Z6FD1) for each robotic twin to measure the net thrust along the front–back distance. The signal is magnified by an amplifier (Maranon load cell transmitter). Since the load cell can measure only the net force instead of the pure generated thrust, we collect static drag as an estimate of the drag experienced by the robot while swimming in the flow tank. The
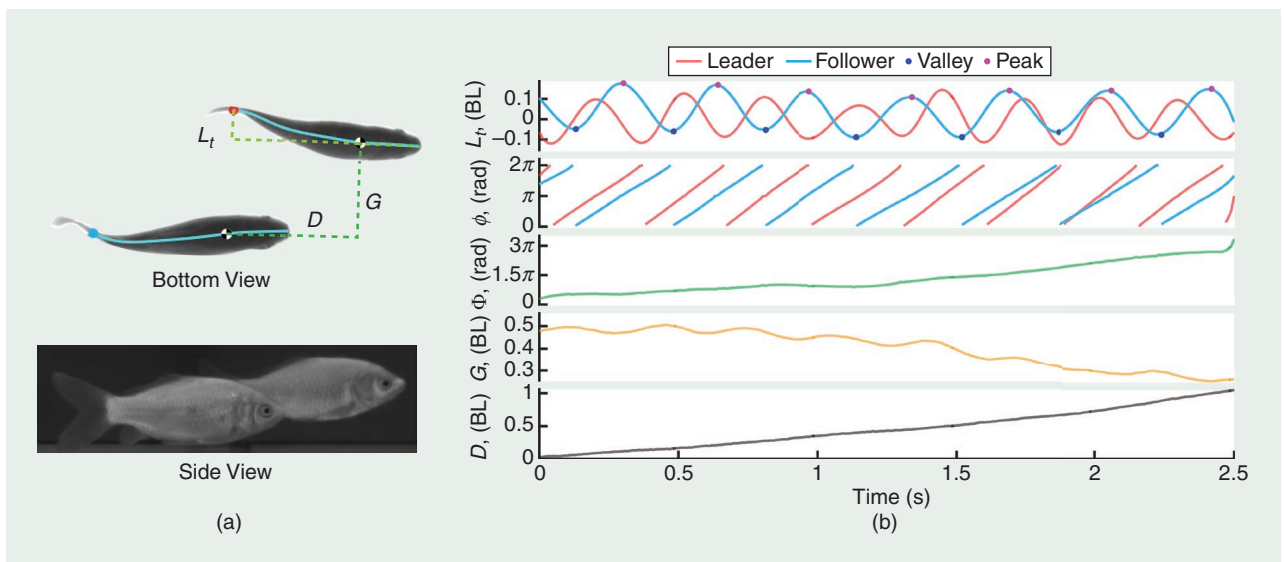

FIGURE 2. (a) and (b) The position and posture information of real fish extracted from the bottom and side views. Posture and position in the *x/y*-axes are mainly determined from the bottom view, the relationship along the *z*-axis is determined from the side view. Relative positions (left–right, *G*, and front–back distances, *D*) between two fish are extracted. The phase difference, Φ, is estimated based on the lateral distance of the tail tip over the center of the fish body, L_t.

thrust, T_{thrust}, is estimated by the resultant force, $T_{\text{resultant}}$, adding the static drag, T_{drag}

$$T_{\text{thrust}} = T_{\text{resultant}} + T_{\text{drag}} \qquad (2)$$

where T_{drag} is measured by evaluating the drag experienced by the static robot under the same incoming flow conditions as in the case of real fish swimming. The sign of all three variables depends on their respective directions. For instance, the drag force is negative, whereas the thrust is positive.

EXPERIMENTS WITH A REAL FISH SYSTEM

To verify the effectiveness of the platform, we employed goldfish (*Carassius auratus*) as a biological model since we found that they employ hydrodynamic interactions while swimming together [8]. Following our previous studies, we use fish with a body size of around 15 cm to increase the potential for hydrodynamic interactions while allowing sufficient space for schooling in our flow tank. The flow speed is set in relation to the body length (BL) to 1.2–1.6 body lengths per second (BLs/s) with an interval of 0.1 BLs/s, which is within the range of their natural speeds [19]. Before the experiments, we first allowed the fish to become accommodated to the flow tank environment for 30 min. For the experiments conducted here, we randomly selected the flow speed and collected fish schooling at that flow speed for approximately 5 min. After this recording, the fish received a minimum of 5 min of rest. This procedure was repeated for 3 h. (Experimental procedures were approved by Regierungspräsidium Freiburg, 35-9185.81/G-17/90.)

From the videos (both bottom and side views), we tracked both 3D positions and 2D postures of the real fish [see Figure 2(a)].

FIGURE 3. Examples of speed graphs for (a) the *x*- and *y*-axis for a leader and a follower and (b) tail movement control. The angle is defined by the deviation of the tail tip from the fish's central body axis. Deg.: degree.

With deep learning, we first received the 2D positions of each fish from both bottom and side views [Figure 2(b)]. The 3D positions were reconstructed based on the calibrated camera matrix. Fish postures were estimated from the bottom view. From the tail tip movement relative to the center line of the fish body L_t, we can detect the peaks and valleys of L_t to determine the tailbeat phase of each robot according to the following transform:

$$\phi = 2\pi \frac{L_t - L_{t(\text{valley})}}{L_{t(\text{peak})} - L_{t(\text{valley})}} \qquad (3)$$

where $L_{t(\text{valley})}$ and $L_{t(\text{peak})}$ are the valley and peak of the lateral tail tip, respectively. The phase ϕ is periodic within $[0, 2\pi]$. According to the phase values, we determined the tail flapping control of the robotic twins (Figures 2 and 3).

From the estimated positions and postures of each real fish, we calculate the swimming speed in *x*-, *y*-, and *z*-dimensions [see Figure 3(a) as well as the tailbeat offsets in Figure 3(b)]. The *x*-axis is the flow direction, and negative values correspond to the fish moving backward with respect to the frame of reference of the camera. Considering the reaction time of the step motors, we averaged the moving speed in *x*, *y*, and *z* in different directions every 0.1 s. For the tailbeat control, we increased the update rate to 100 times per second to minimize the deviation between the amplitudes of real and robotic fish. Due to inevitable small tracking errors, we smoothed the speeds utilized for position control and tailbeats using a moving average with a window size of five.

POWER COST, THRUST, AND THRUST EFFICIENCY OF SCHOOLING FISH

To mutually verify the RoboTwin platform and our previously proposed vortex phase matching rule [8], we collected data where there exist a clear leader and follower, and they are sufficiently close (smaller than 0.5 BLs) such that the follower could be expected to be able to benefit from the hydrodynamic interactions. To replicate the movements of the two real fish, we programmed the RoboTwin to reproduce the dynamic body kinematics and body movements. Subsequently, we measured the power expenditure and thrust generated by the RoboTwin. To gain further insights, we also conducted flow visualizations using PIV to explore the nature of the hydrodynamic interactions. As controls, we further conducted experiments with the follower swimming alone and swimming in the same group but with an opposite tail beat phase compared to the observed real fish. This allowed us to comprehensively assess the platform's performance and analyze the potential benefits of swimming together in fish.

ESTIMATING POWER COST AND THRUST

We gathered data on the power cost and thrust of the follower robot as it replicated the dynamic relative formations and body kinematics of both fish. Based on our previous studies [8], we expected the follower to save energy through a mechanism termed *vortex phase matching*. The tailbeat of the follower matches the nearby vortex shed by the leading
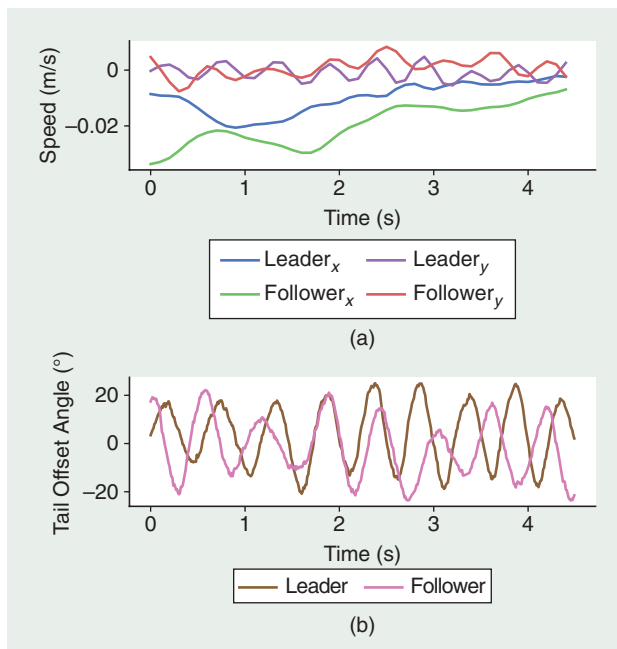
individual regardless of the front–back distance. We first converted the lateral distance of the tail tip extracted from the tracking step to the tailbeat angle for the servomotor within the robot (Figure 4). Figure 4 provides a comparison between two real fish swimming in a flow tank and the RoboTwin reproducing their movements within the same environment. Despite having a single joint, the central line of the robot's movement closely resembles that of the real fish (refer to supplementary video for a detailed comparison).

Figure 5 presents the power cost and thrust data obtained from one of the robotic twins. The robot exhibits a sinusoidal wave motion with an amplitude of 25° and a frequency of 2 Hz over a duration of 10 s. Due to the collection of power cost and thrust data at a high frame rate (5,000 Hz), we applied a mov-
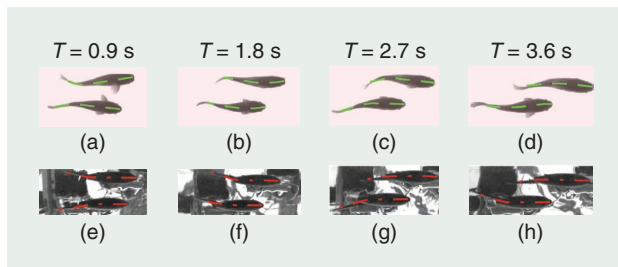
ing average smoothing algorithm with a window size of 100 (equivalent to 10 ms in real time). This allowed us to visualize the changes in power cost and thrust within the same time window as the tailbeat movement (Figure 5). It is evident from the data that the power cost and thrust exhibit synchronous variations, occurring predominantly at twice the frequencies of the tail movements. This is due to the fact that the power cost and thrust values align when the tail reaches its leftmost and rightmost positions, thus verifying our power cost and thrust measuring system.

THE IMPACT OF HYDRODYNAMIC INTERACTIONS

To investigate the potential benefits of swimming together for schooling fish, we conducted a comparative analysis of swimming performance metrics, including power cost, thrust, and thrust efficiency, between robotic fish swimming in groups and swimming alone. Figure 6 shows the instantaneous power costs and thrusts in relation to tailbeat flapping. We observe that as the amplitude increases, the power costs increase. The moment when the real fish's tail reaches its leftmost position is highlighted with dashed lines as a reference time. When comparing the power costs of the follower swimming alone versus swimming together with a leader, we observed that the

FIGURE 4. A comparison of the spatiotemporal movements and body kinematics of (a)–(d) real and (e)–(h) robotic schooling fish at different times.
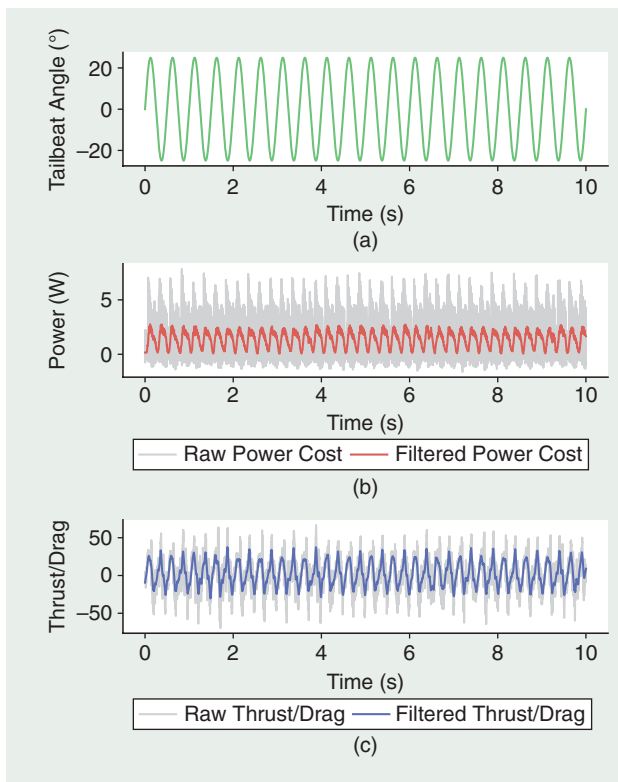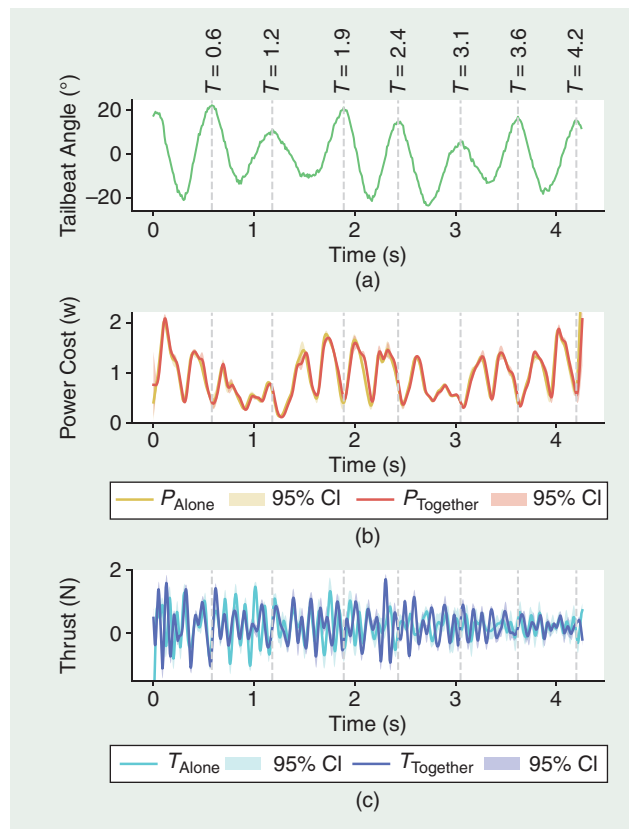

FIGURE 5. Examples of power cost and thrust over time under an idealized sinusoidal body undulation. (a) The robot's tailbeat exhibits a sinusoidal wave motion with an amplitude of 25° and a frequency of 2 Hz. (b) and (c) The corresponding (b) power cost over hydrodynamics and (c) thrust over drag as functions of time.

FIGURE 6. (a) The power costs and (b) the corresponding thrusts generated by the follower when swimming alone or together with the leader, replicating the movements and kinematics of actual fish. The shaded error represents a 95% confidence interval. The moment when the follower reaches the leftmost position is indicated, corresponding to our subsequent flow visualization analysis in Figure 8.

follower employs less energy and increases thrust after 2 s when swimming together. This finding aligns with the concept of vortex phase matching, as detailed in the flow visualization analysis presented later.

Figure 7 illustrates the power cost, thrust, and thrust efficiency of a follower fish in three scenarios: 1) swimming in
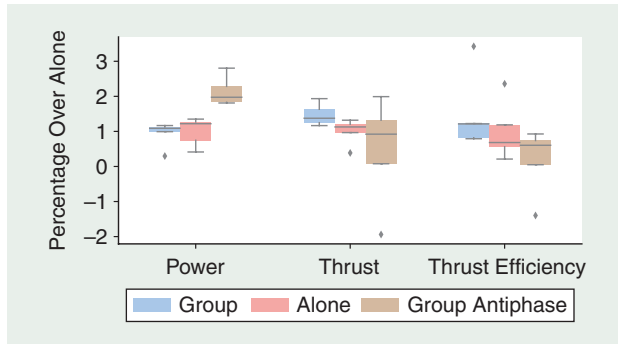

FIGURE 7. A comparison evaluates the power costs, thrusts, and thrust efficiency of a follower fish in three scenarios: 1) swimming in tandem with a leader in the same spatial formation and phase, as observed in real fish; 2) swimming alone; and 3) swimming alongside a leader in the same spatial formation but in antiphase. The values are normalized based on the average power cost, thrust, and thrust efficiency when the robot swims alone. The experiment gathered more than 22,500 data points for power cost and thrust. It was conducted five times, both for collective swimming and individual swimming.
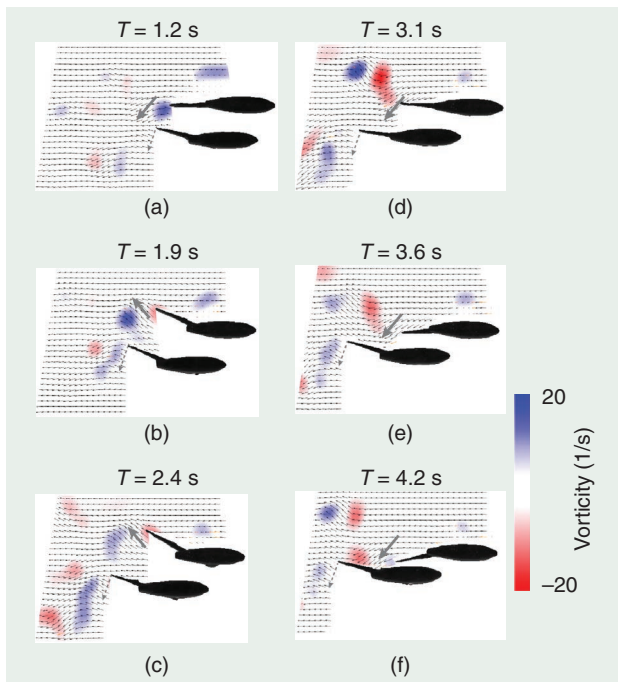

FIGURE 8. (a)–(f) An estimation of the hydrodynamic interactions between two real fish using our RoboTwin platform and PIV technique. In the visual representation, arrows indicate the velocity of the flow at each spatial position. Additionally, the color-coded visualization depicts the vorticity along the z-axis, where red represents clockwise rotation and blue represents counterclockwise rotation. The induced flow direction is marked with a solid gray arrow, and the tailbeat direction is marked with a dashed gray arrow.

tandem with a leader in the same phase, as observed in real fish; 2) exhibiting the same motion and kinematics but swimming alone; and 3) swimming alongside a leader in the same spatial formation but in antiphase. After conducting five repetitions for each scenario, we find that the power cost is reduced by 8%, and the thrust of the follower when swimming together as real fish did is improved by around 35%. The thrust efficiency of the follower, which is defined by the thrust over the power cost, is increased by around 63%. The antiphase case requires more energy and does not gain significant thrust, resulting in lower thrust efficiency.

HYDRODYNAMIC INTERACTION VISUALIZATION

To investigate the mechanism behind energy saving and thrust improvement, we employed PIV using our RoboTwin to estimate the hydrodynamic interactions between two real fish. PIV was conducted using polyamic particles (diameter of 100 um) and illuminated with a laser generator (Laserwave, LW532PIV-8W). High-speed videos were captured using a Phantom S991 camera at a resolution of 4K and a frame rate of 200 fps. PIV data analysis was performed using PIVlab [20].

We primarily focused on analyzing the hydrodynamic interactions that occur when the follower starts moving its tail from the leftmost to the right at specific time intervals: t = 1.2, 1.9, 2.4, 3.1, 3.6, and 4.2 s. Our investigation revealed that in cases where the front–back distance between the leader and follower is relatively small, the follower predominantly coordinates with the leader to generate jet flowthrough vortex–vortex interactions [refer to Figure 8(a) and (b)]. This phenomenon could potentially explain the observed improvement in thrust. Furthermore, as depicted in Figure 8(c), the state begins to transition as the follower primarily focuses on energy conservation through vortex phase matching [Figure 8(d)–(f)]. In this state, the follower flaps its tail in the same direction as the incoming induced flow, which we find allows it to save energy. This finding aligns with our previous analyses and provides additional insight (e.g., flow visualization and potential mapping between hydrodynamic inputs and movement decision outputs) into the observed energy-saving phenomenon [8].

CONCLUSION AND DISCUSSIONS

We introduce the RoboTwin platform, which enables the study of hydrodynamic interactions in fish schools. The platform features robotic fish that replicate the realistic morphology, movements, and kinematics of schooling fish. With this setup, we can directly measure the power cost and thrust of each robot, making it easy, fast, and reliable to estimate the impact of hydrodynamic factors on these variables for the kinematics exhibited by real fish. In the future, we plan to use this platform to investigate scenarios in which schooling fish derive benefits from energy savings versus those in which they prioritize thrust improvement.

One limitation of our current RoboTwin platform is that we are limited to a pair of robots. However, this is still biologically

meaningful since the strongest hydrodynamic interactions in fish schools are those with the nearest individuals, and swimming in pairs is the most common configuration found in natural fish populations [2], [3]. For those situations where more real fish are schooling, we will be able to model the situation by subgrouping them according to the nearest distances. Future research will concentrate on more detailed analyses of instantaneous hydrodynamic interactions as well as the advantages and costs to the leader. Additionally, we would also like to explore the dynamics of assuming the role of either leader or follower in group formations. All these would not only shed light on the hydrodynamic mechanisms of schooling fish but also open new avenues for enhancing the design and coordination of underwater robotic systems.

ACKNOWLEDGMENT

AUTHORS

Liang Li, Department of Collective Behavior, Max Planck Institute of Animal Behavior, 78464 Konstanz, Germany, Centre for the Advanced Study of Collective Behavior, University of Konstanz, Konstanz, Germany, and Department of Biology, University of Konstanz, Konstanz, Germany. E-mail: lli@ab.mpg.de and liang.li@uni-konstanz.de.

Li-Ming Chao, Department of Collective Behavior, Max Planck Institute of Animal Behavior, 78464 Konstanz, Germany, Centre for the Advanced Study of Collective Behavior, University of Konstanz, 78457 Konstanz, Germany, and Department of Biology, University of Konstanz, 78457 Konstanz, Germany. E-mail: lchao@ab.mpg.de.

Siyuan Wang, Department of Collective Behavior, Max Planck Institute of Animal Behavior, 78464 Konstanz, Germany, Centre for the Advanced Study of Collective Behavior, University of Konstanz, 78457 Konstanz, Germany, and Department of Biology, University of Konstanz, 78457 Konstanz, Germany. E-mail: wsydlmu@dlmu.edu.cn.

Oliver Deussen, Centre for the Advanced Study of Collective Behavior, University of Konstanz, 78457 Konstanz, Germany, and Department of Computer and Information Science, University of Konstanz, 78457 Konstanz, Germany. E-mail: deussen@inf.uni-konstanz.de.

Iain D. Couzin, Department of Collective Behavior, Max Planck Institute of Animal Behavior, 78464 Konstanz, Germany, Centre for the Advanced Study of Collective Behaviour, University of Konstanz, 78457 Konstanz, Germany, and Department of Biology, University of Konstanz, 78457 Konstanz, Germany. E-mail: icouzin@ab.mpg.de.

REFERENCES

[1] D. T. Sumpter, *Collective Animal Behavior.* Princeton, NJ, USA: Princeton Univ. Press, 2010.

[2] Y. Katz, K. Tunstrøm, C. C. Ioannou, C. Huepe, and I. D. Couzin, "Inferring the structure and dynamics of interactions in schooling fish," *Proc. Nat. Acad. Sci. USA*, vol. 108, no. 46, pp. 18,720–18,725, 2011, doi: 10.1073/pnas.1107583108.

[3] S. B. Rosenthal, C. R. Twomey, A. T. Hartnett, H. S. Wu, and I. D. Couzin, "Revealing the hidden networks of interaction in mobile animal groups allows prediction of complex behavioral contagion," *Proc. Nat. Acad. Sci. USA*, vol. 112, no. 15, pp. 4690–4695, 2015, doi: 10.1073/pnas.1420068112.

[4] D. Weihs, "Hydromechanics of fish schooling," *Nature*, vol. 241, no. 5387, pp. 290–291, 1973, doi: 10.1038/241290a0.

[5] J. Deng, X.-M. Shao, and Z.-S. Yu, "Hydrodynamic studies on two traveling wavy foils in tandem arrangement," *Phys. Fluids*, vol. 19, no. 11, Nov. 2007, Art. no. 113104, doi: 10.1063/1.2814259.

[6] L.-M. Chao, G. Pan, D. Zhang, and G.-X. Yan, "On the thrust generation and wake structures of two travelling-wavy foils," *Ocean Eng.*, vol. 183, pp. 167–174, Jul. 2019, doi: 10.1016/j.oceaneng.2019.04.097.

[7] L.-B. Jia and X.-Z. Yin, "Passive oscillations of two tandem flexible filaments in a flowing soap film," *Physical Rev. Lett.*, vol. 100, no. 22, 2008, Art. no. 228104, doi: 10.1103/PhysRevLett.100.228104.

[8] L. Li, M. Nagy, J. M. Graving, J. Bak-Coleman, G. Xie, and I. D. Couzin, "Vortex phase matching as a strategy for schooling in robots and in fish," *Nature Commun.*, vol. 11, no. 1, 2020, Art. no. 5408, doi: 10.1038/s41467-020-19086-0.

[9] H. Hamann, *Swarm Robotics: A Formal Approach.* Cham, Switzerland: Springer-Verlag, 2018.

[10] L. E. Nadler, S. S. Killen, E. C. McClure, P. L. Munday, and M. I. McCormick, "Shoaling reduces metabolic rate in a gregarious coral reef fish species," *J. Exp. Biol.*, vol. 219, no. 18, pp. 2802–2805, 2016, doi: 10.1242/jeb.139493.

[11] S. Verma, G. Novati, and P. Koumoutsakos, "Efficient collective swimming by harnessing vortices through deep reinforcement learning," *Proc. Nat. Acad. Sci. USA*, vol. 115, no. 23, pp. 5849–5854, 2018, doi: 10.1073/pnas.1800923115.

[12] L. Ristroph and J. Zhang, "Anomalous hydrodynamic drafting of interacting flapping flags," *Physical Rev. Lett.*, vol. 101, no. 19, 2008, Art. no. 194502, doi: 10.1103/PhysRevLett.101.194502.

[13] A. D. Becker, H. Masoud, J. W. Newbolt, M. Shelley, and L. Ristroph, "Hydrodynamic schooling of flapping swimmers," *Nature Commun.*, vol. 6, no. 1, 2015, Art. no. 97, doi: 10.1038/ncomms9514.

[14] L. Li, S. Ravi, G. Xie, and I. D. Couzin, "Using a robotic platform to study the influence of relative tailbeat phase on the energetic costs of side-by-side swimming in fish," *Proc. Roy. Soc. A*, vol. 477, no. 2249, May 2021, Art. no. 20200810.

[15] J. M. Graving et al., "DeepPoseKit, a software toolkit for fast and robust animal pose estimation using deep learning," *eLife*, vol. 8, Oct. 2019, Art. no. e47994, doi: 10.7554/eLife.47994.

[16] A. Mathis et al., "DeepLabCut: Markerless pose estimation of user-defined body parts with deep learning," *Nature Neurosci.*, vol. 21, no. 9, pp. 1281–1289, 2018, doi: 10.1038/s41593-018-0209-y.

[17] R. Wu, O. Deussen, and L. Li, "DeepShapeKit: Accurate 4D shape reconstruction of swimming fish," in *Proc. IEEE/RSJ Int. Conf. Intell. Robots Syst. (IROS)*, 2022, pp. 526–531, doi: 10.1109/IROS47612.2022.9982097.

[18] L. Li, C. Wang, and G. Xie, "A general CPG network and its implementation on the microcontroller," *Neurocomputing*, vol. 167, pp. 299–305, Nov. 2015, doi: 10.1016/j.neucom.2015.04.066.

[19] W. Hanke, C. Brucker, and H. Bleckmann, "The ageing of the low-frequency water disturbances caused by swimming goldfish and its possible relevance to prey detection," *J. Exp. Biol.*, vol. 203, no. 7, pp. 1193–1200, 2000, doi: 10.1242/jeb.203.7.1193.

[20] W. Thielicke and R. Sonntag, "Particle image velocimetry for MATLAB: Accuracy and enhanced algorithms in PIVlab," *J. Open Res. Softw.*, vol. 9, no. 1, 2021, Art. no. 12, doi: 10.5334/jors.334.